Study case on Miyakejima volcano (Japan), by combining MT, seismicity, thermal image (remote sensing), and self-potential

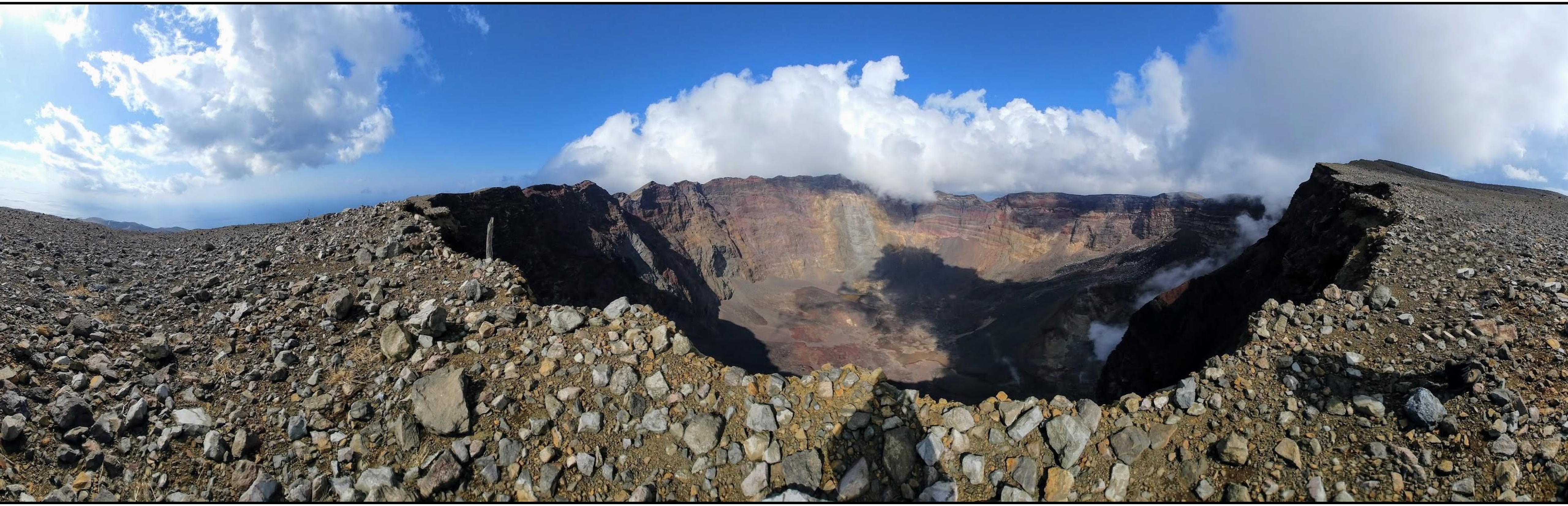

Presented by Marceau GRESSE

Gresse et al., (2021), JGR SE

10.1029/2021JB022034

東京大学 THE UNIVERSITY OF TOKYO

JSPS

EARTHQUAKE RESEARCH INSTITUTE

*marceau.gresse@gmail.com

Motivation: better understand magmatic-hydrothermal interactions

Hydrothermal systems = **water** and **heat transfer** through porous/fractured **rocks**

Magmatic-hydrothermal interactions

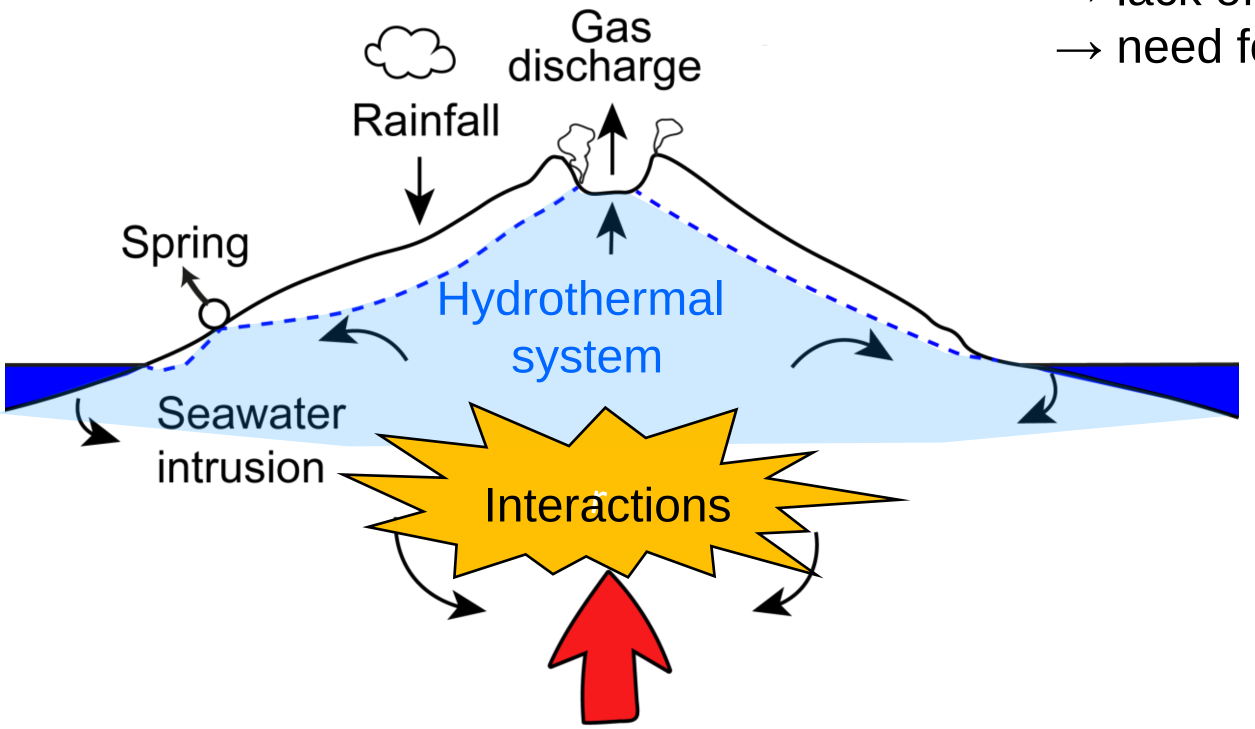

- **1. Hazards:** phreatic, phreato-magmatic eruptions, landslide
  → **high-risk** in populated areas
- **2. Problem: difficult to forecast** hydrothermal-related hazards
  → lack of large-scale understanding
  → need for multidisciplinary approaches

Phreatomagmatic event
Miyakejima, 15 July 2000
(Nakada et al., 2005)

Study area: Miyakejima volcano

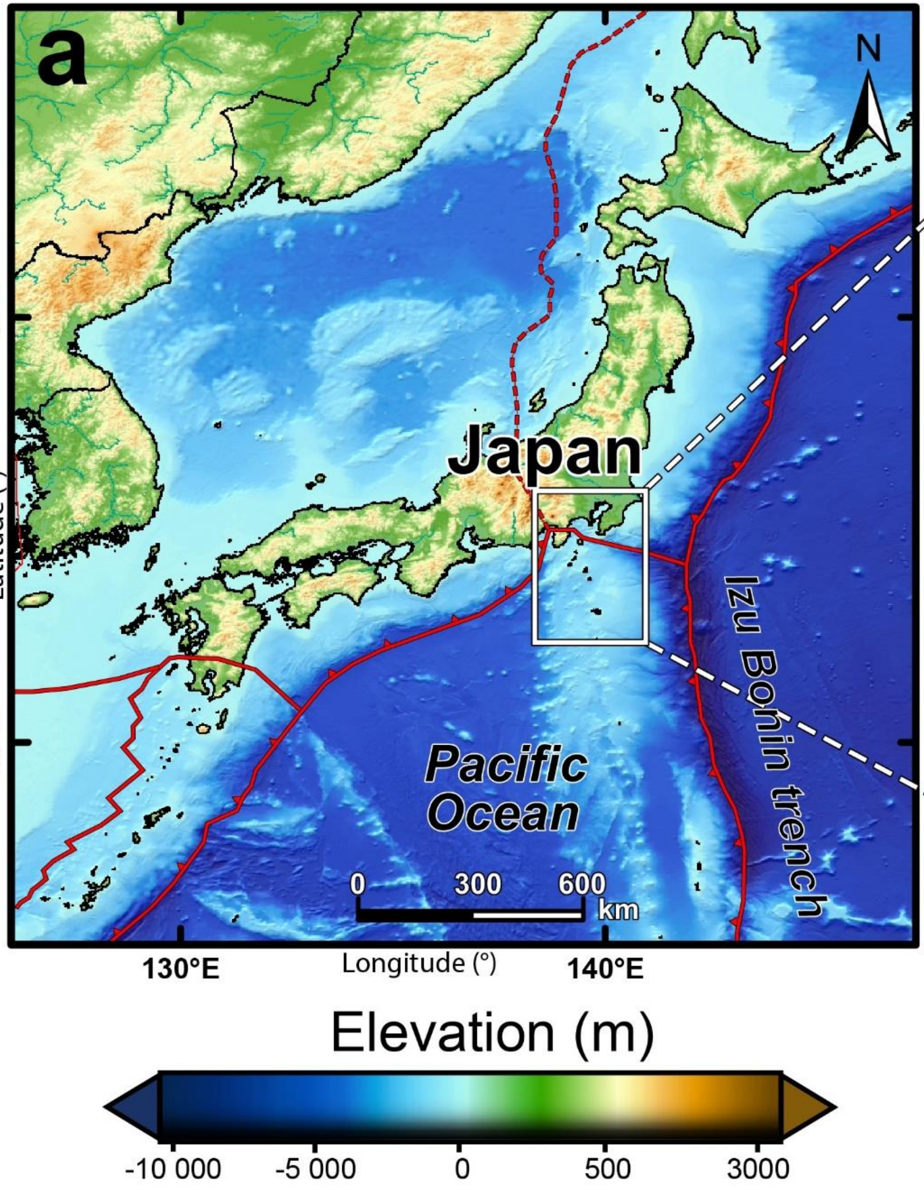

200 km to the South of Tokyo

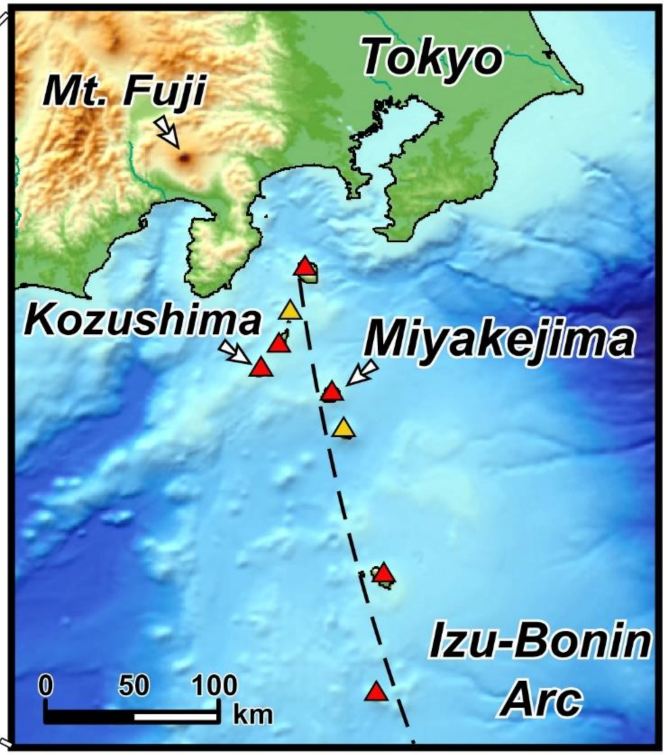

Miyakejima

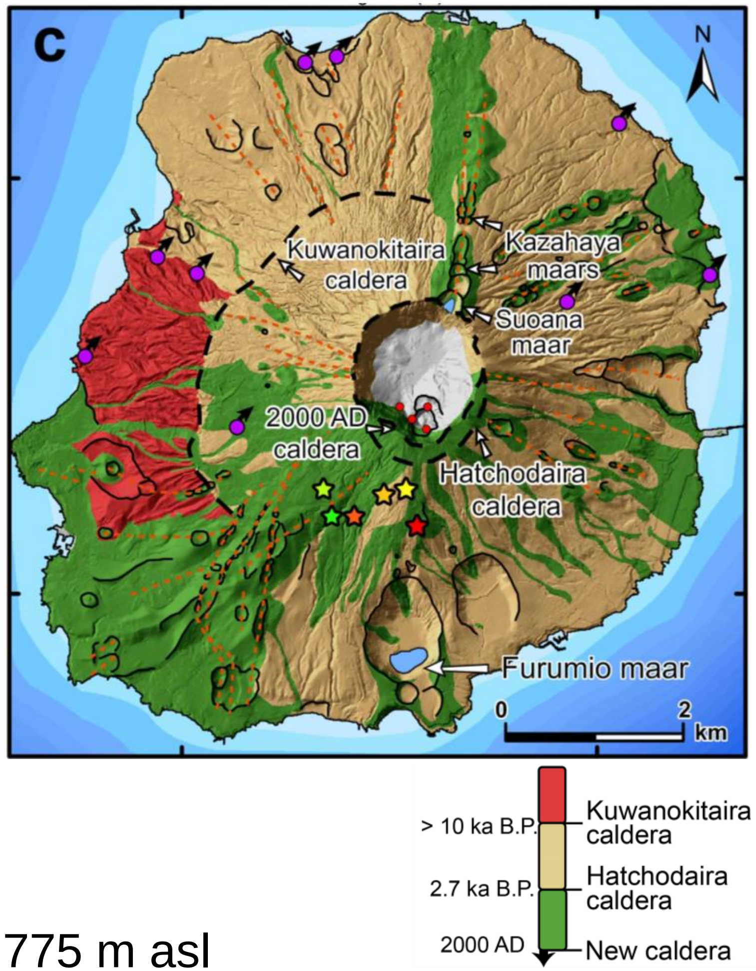

- Extensive hydrothermal system
- Small stratovolcano, 10-km wide, 775 m asl
- Regular eruptions ~20 years: 1940, 1962, 1983, 2000…?

Study area: Miyakejima volcano: 2000 A.D. eruption

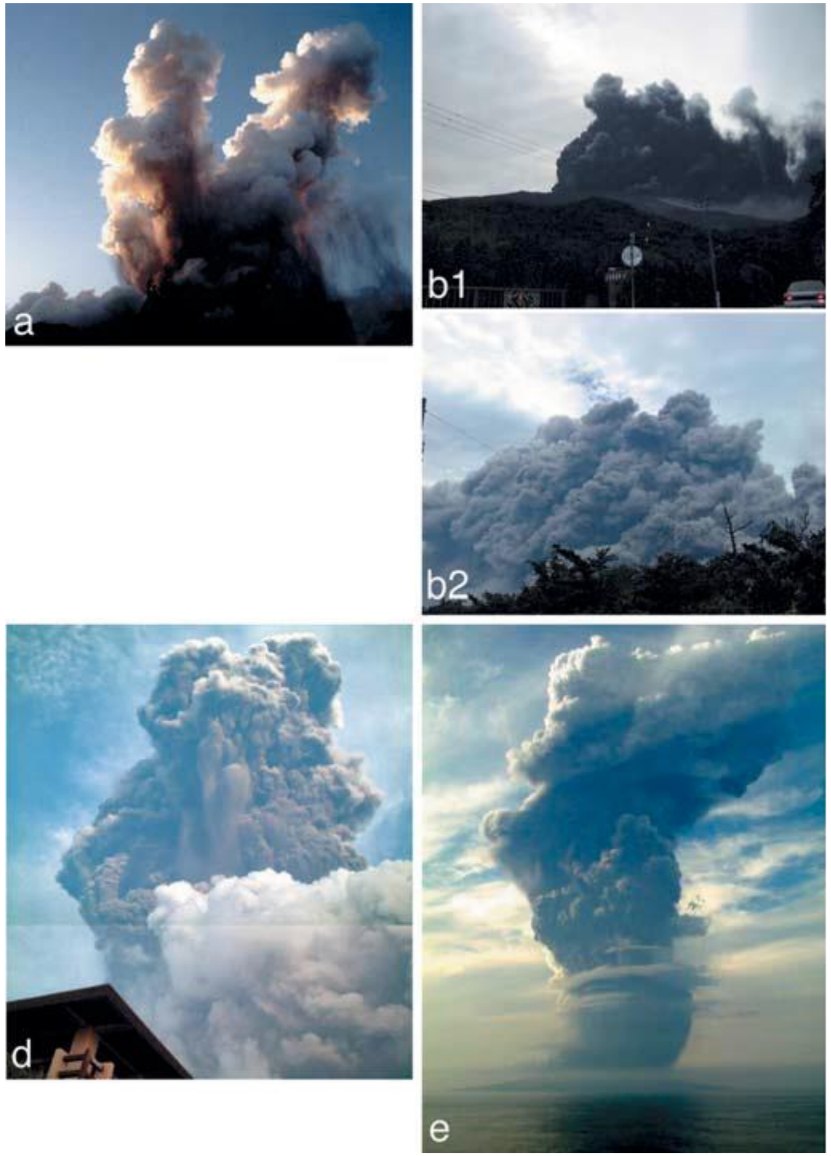

Phreatic-phreatomagmatic eruption, Miyakejima, July-August 2000 (Nakada et al., 2005)

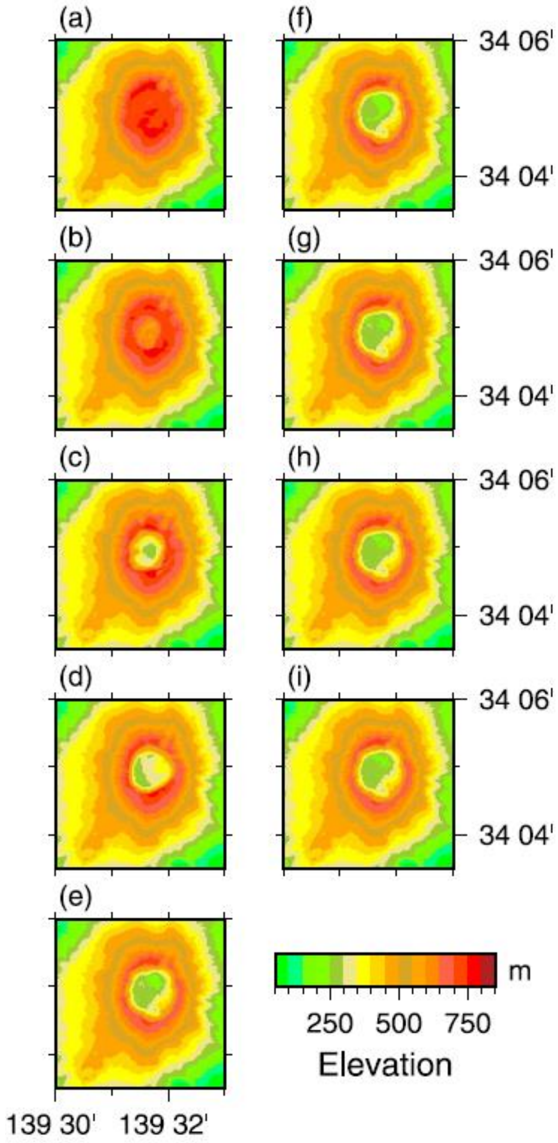

Temporal evolution of collapsed caldera at Miyakejima volcano (Furuya et al., 2003)

Objective of this study

First large-scale imagery of Miyakejima plumbing system

- **Delineate water-rich zones, fluid circulation, and magmatic-hydrothermal interactions**

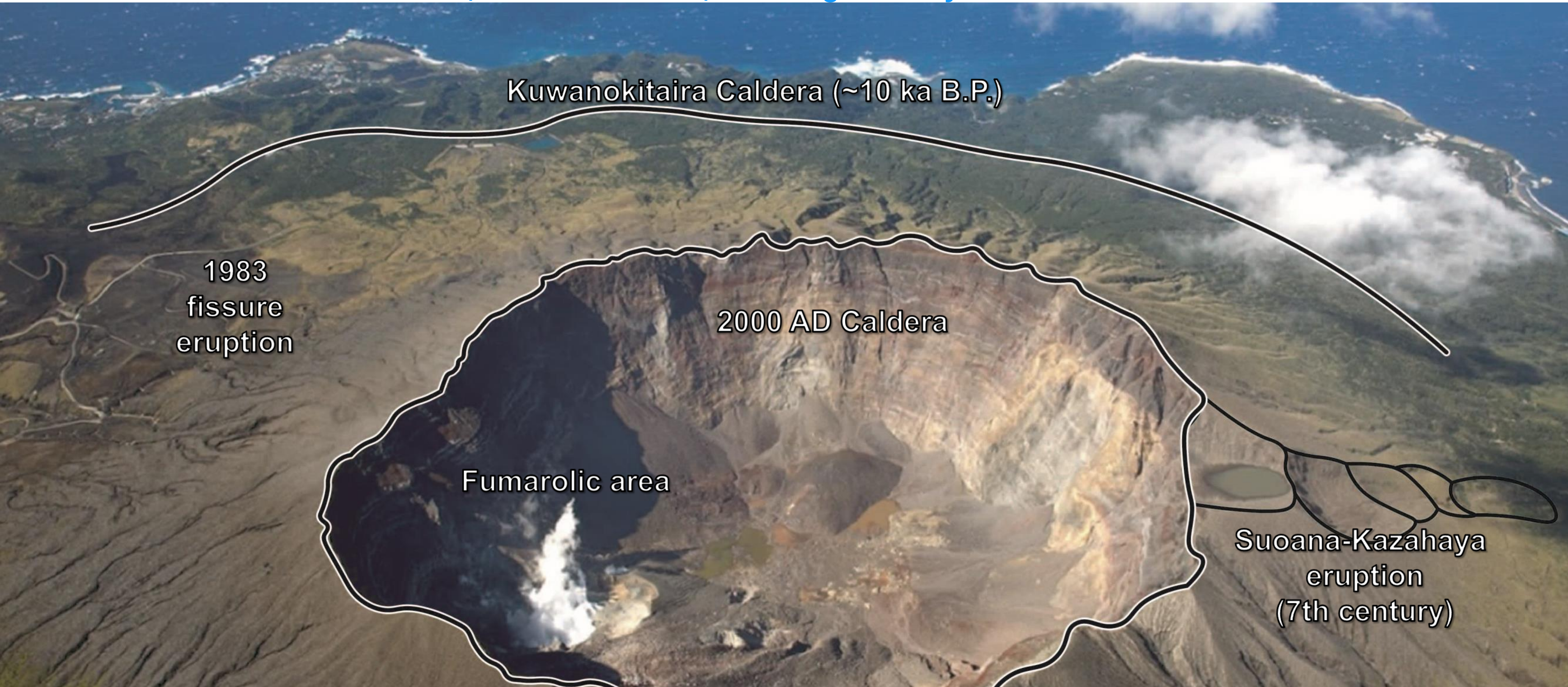

Objective of this study

First large-scale imagery of Miyakejima plumbing system

- **Delineate water-rich zones, fluid circulation, and magmatic-hydrothermal interactions**

Multidisciplinary approach: 4 geophysical methods

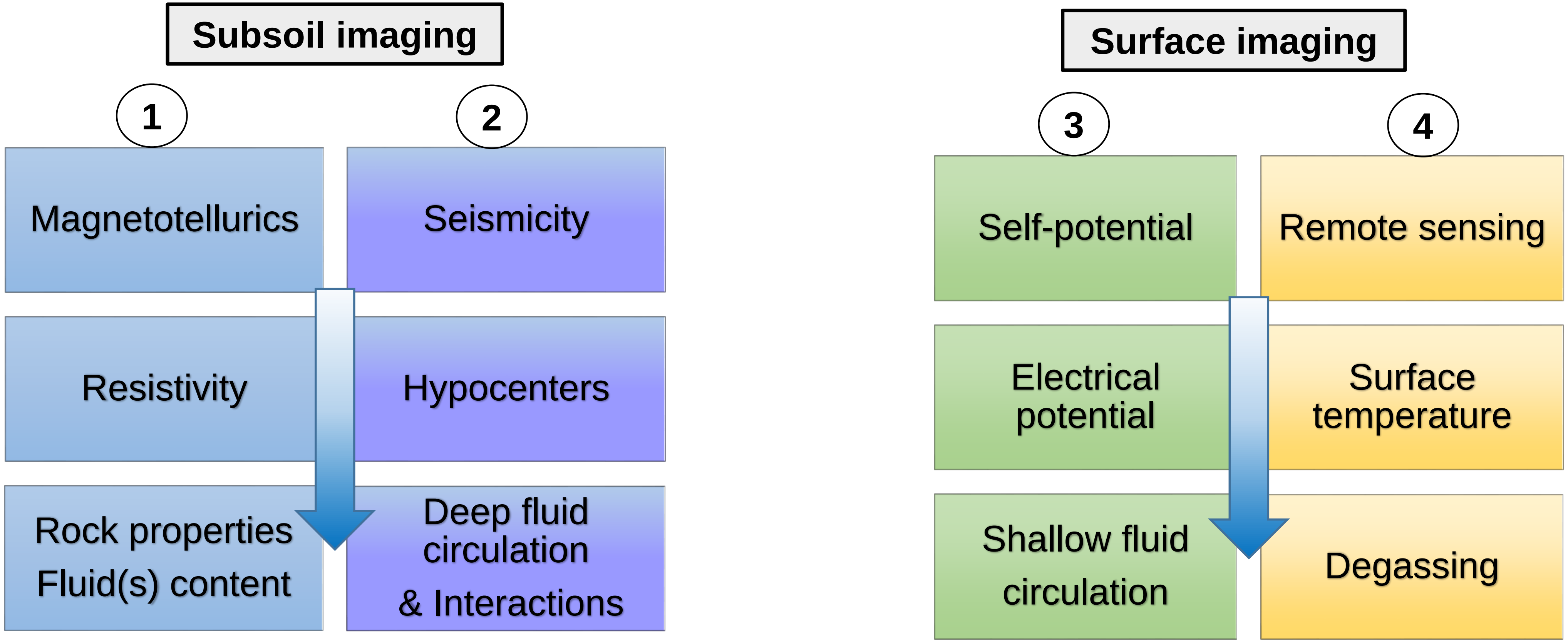

Subsoil imagery (1): Magnetotellurics

MT sites: 13 broadband stations, 2012 (June-August)

Processing: ***Z*** and ***T*** transfer functions with BIRRP *(Chave & Thomson, 2004)*

17 periods between [10^{-2} - 10^{3}] s

Model space: 398,239 elements (200 km^3, 71 × 71 × 79 cells in *x*, *y*, and *z* direction)

Inversion: Occam's type, WSINV3DMT code *(Siripunvaraporn and Egbert, 2009)*

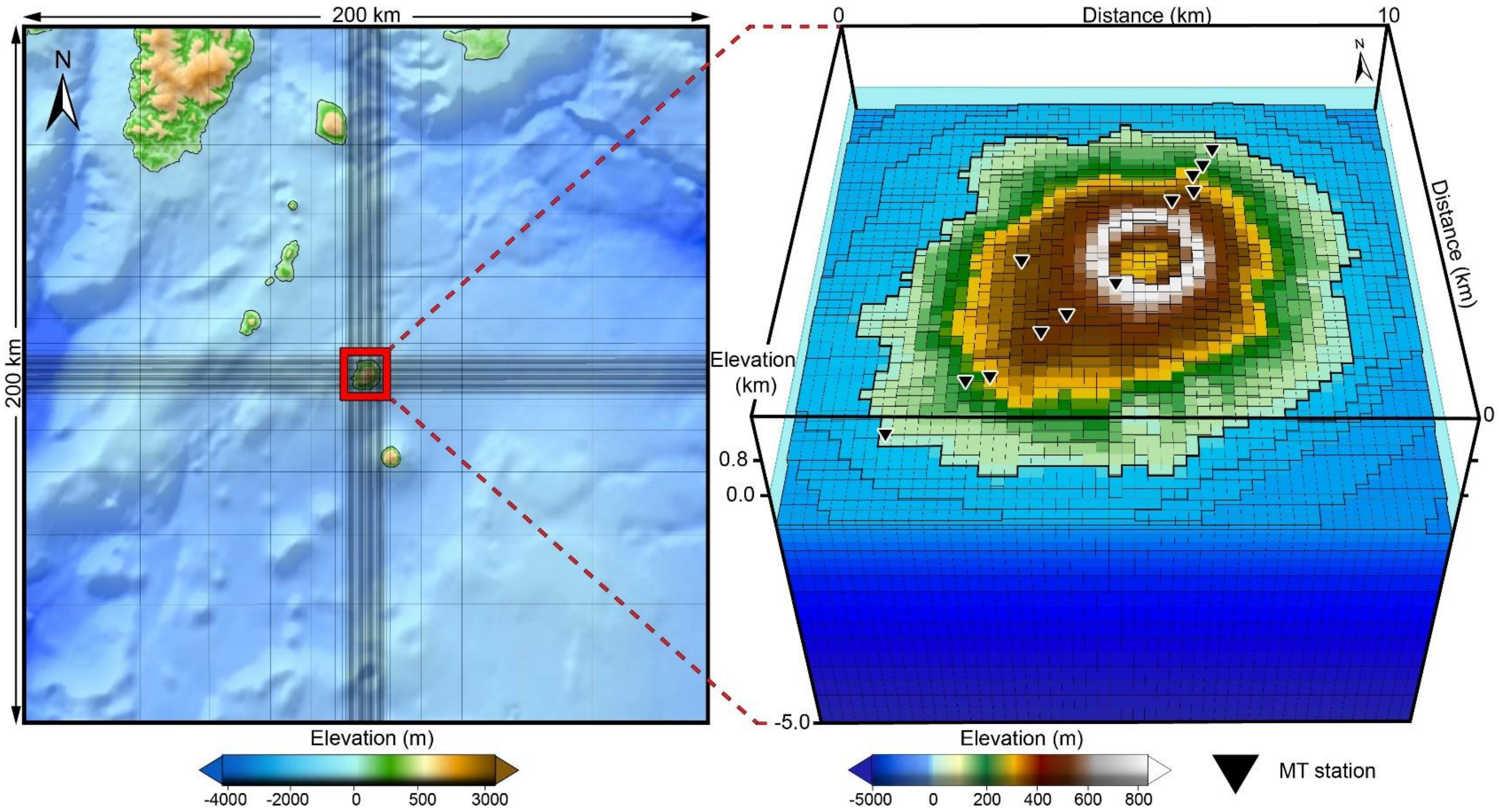

Minimum mesh size
X Y = 200 m
Z = 30 m

Subsoil imagery (2): Seismicity

5 seismometers: 3-components, 100 Hz sampling rate, NIED network

Processing: nonlinear maximum-likelihood algorithm *(Hirata and Matsu'ura, 1987)* *(performed by NIED, Tsukuba)*

Hypocenters classification:

- Long-period (LP) (1-5 Hz)
- Hybrid (3-9 Hz)
- Volcano-tectonic (VT) (5-15 Hz)

Periods selected:

2001.9→2012.9 VT: degassing activity after 2000 eruption

2011.9→2012.9 LP+Hybrid: covers the entire surveys of this study

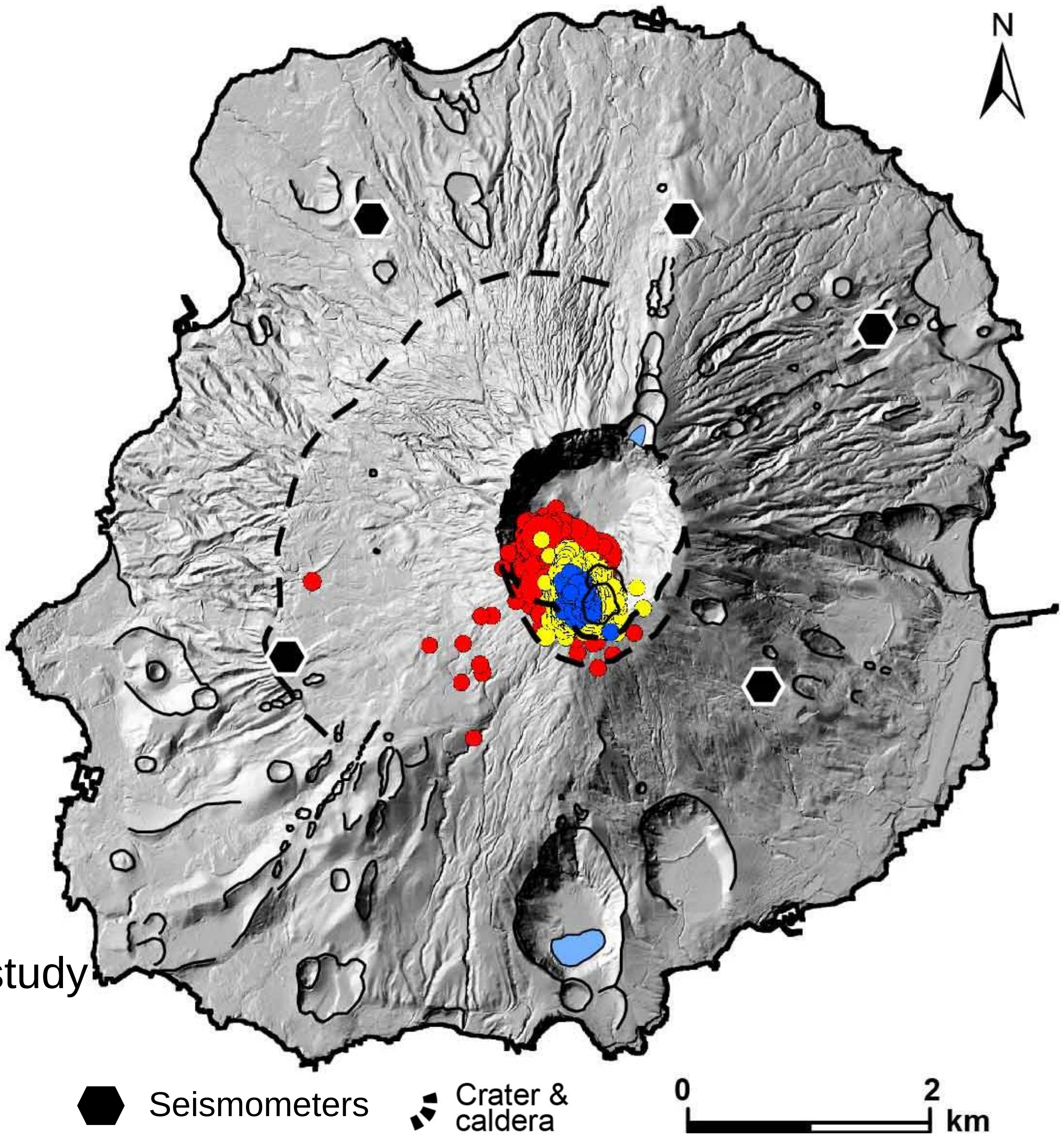

Surface imaging (1): Self-potential

Equipment: non-polarizable Cu-$CuSO_4$ electrodes

3 self-potential profiles:

South line ● 78 pts (2011.9)

North line ● 71 pts (2011.11)

Middle line ● 71 pts (2012.6)

➢ North and South line merged

Reference point:

Southernmost site at 0 mV

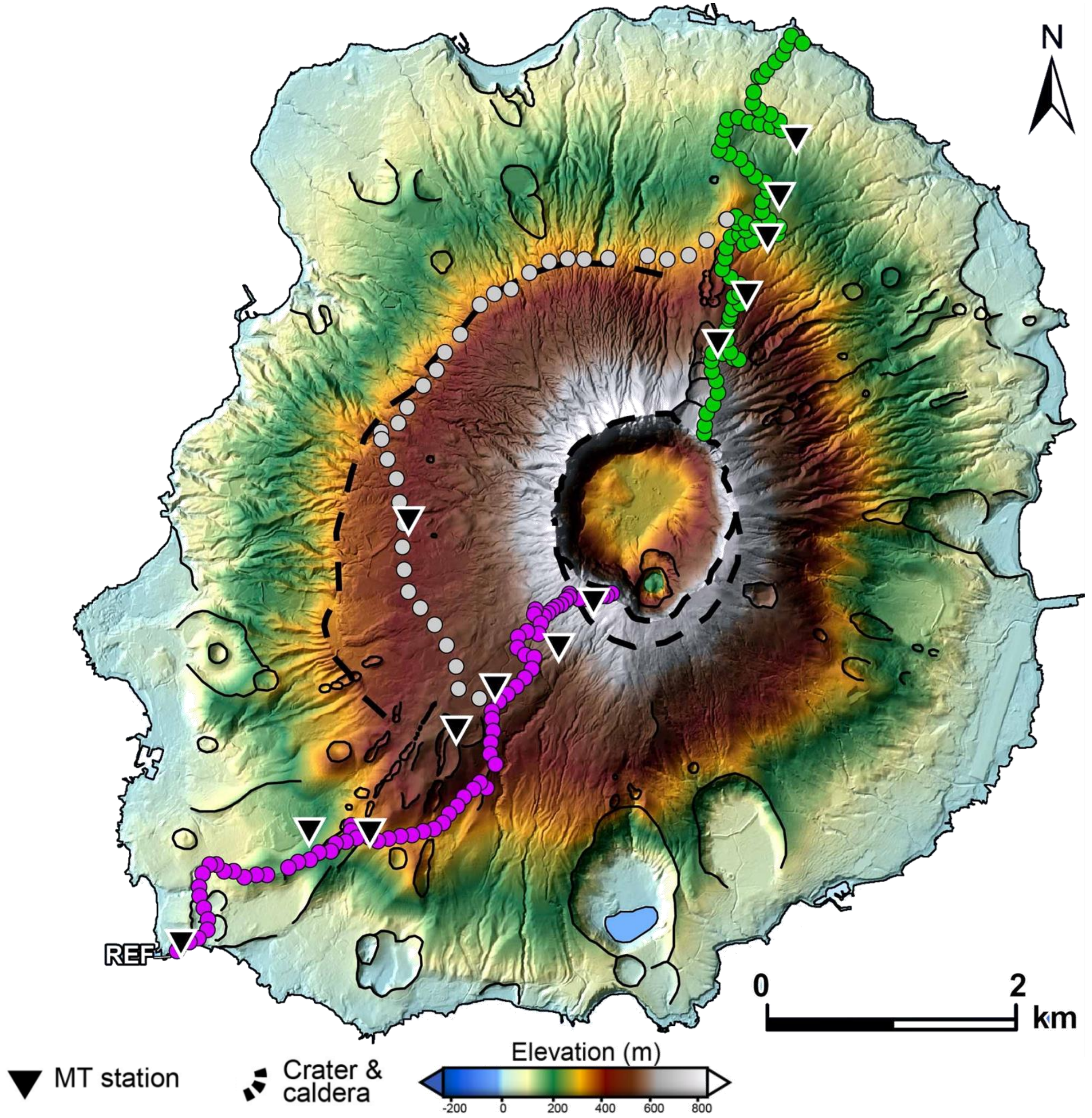

Surface imaging (2): Remote sensing

Infrared spectral radiance images:

ASTER (TIR band 14) [- 30 – + 50°C] 90-m resolution 2011/11/23 (day)

Landsat 7 (SWIR band 7) [+ 90 – + 260°C] 30-m resolution 2012/01/31 (night)

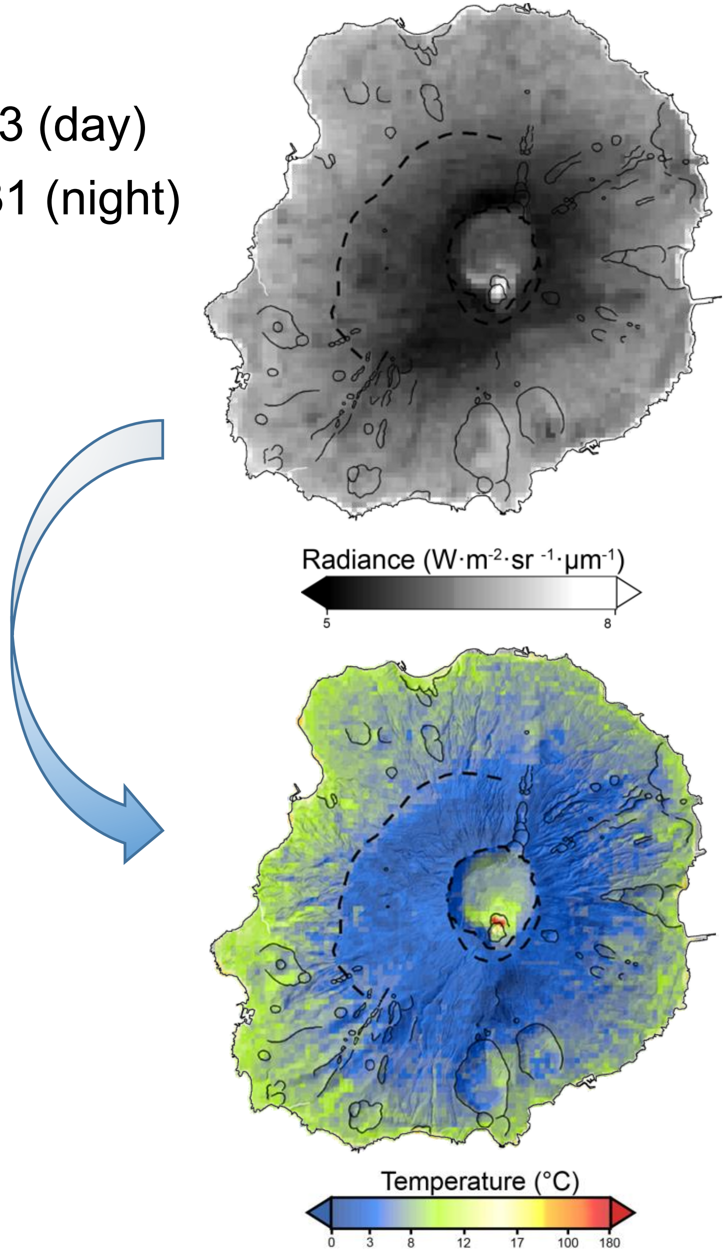

Processing

Atmospheric corrections (transmittance, *up-welling radiance) MODTRAN*

Vegetation cover

Soil emissivity *(Sobrino et al.,1990)*

Inverse Planck function

$$t(\lambda) = \frac{c_2}{\lambda \cdot ln\left(\frac{c_1 \lambda^{-5} \cdot}{R(\lambda)} + 1\right)}$$

Validation

Temperature validated with *in situ* measurements

Results: surface temperature

SW-NE Cross-section along MT stations

Topography draped with surface temperature

Caldera fissures-faults

MT stations

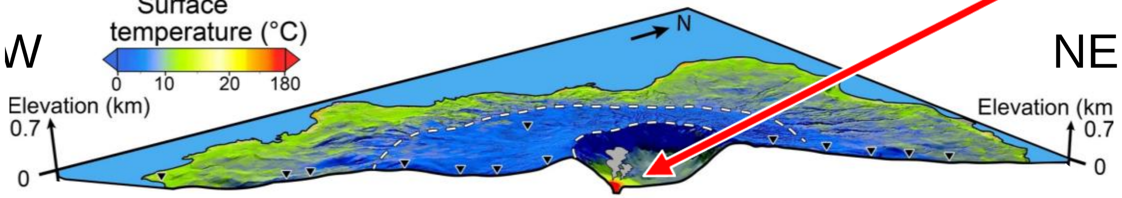

Fumarolic area at 181 °C (2012)

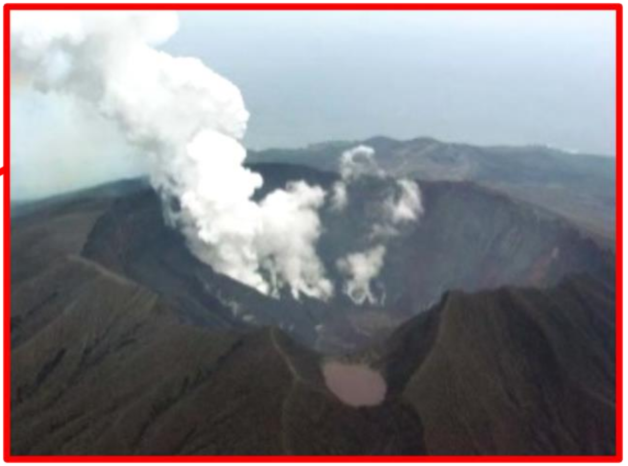

(~370 °C in 2000-2006)

Results: resistivity model, RMS, apparent resistivity, and phase

Occam's style inversion: 7 iterations, final RMS = 1.76

Final error floor Z= 15 %, T= 20 %

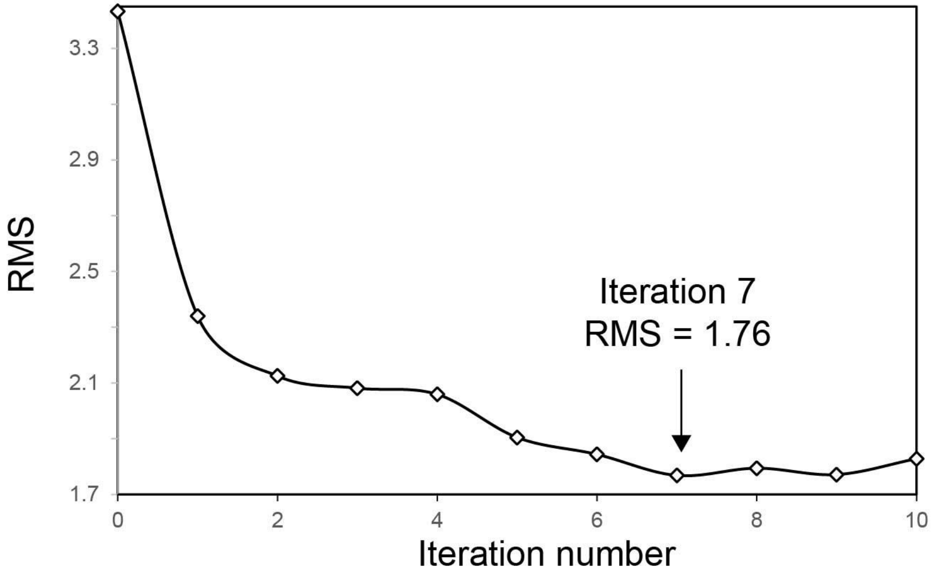

Conductor

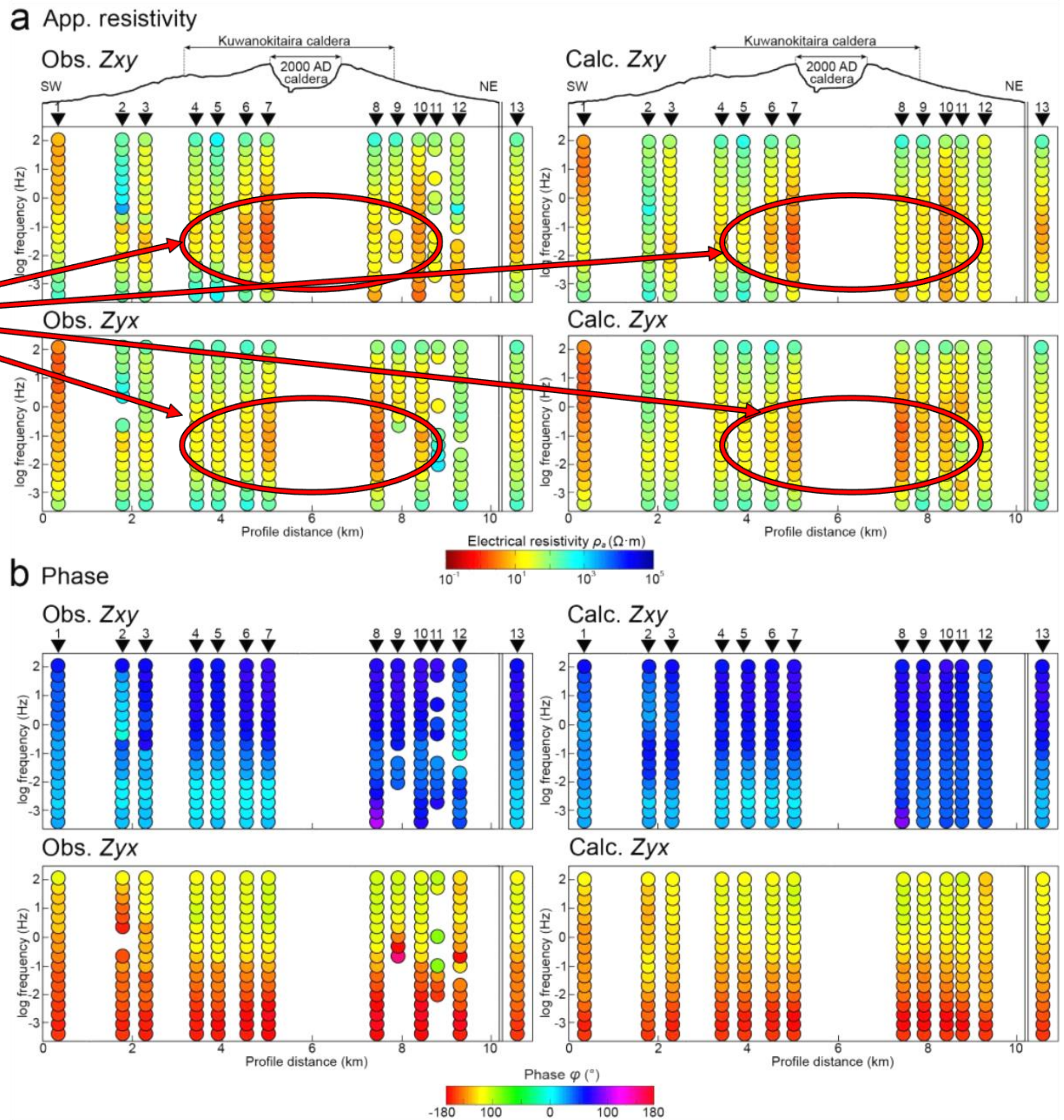

Good agreement between observed and calculated ap. resistivity and phase

Results: resistivity model, induction vectors $\vec{T}real\,(f)$

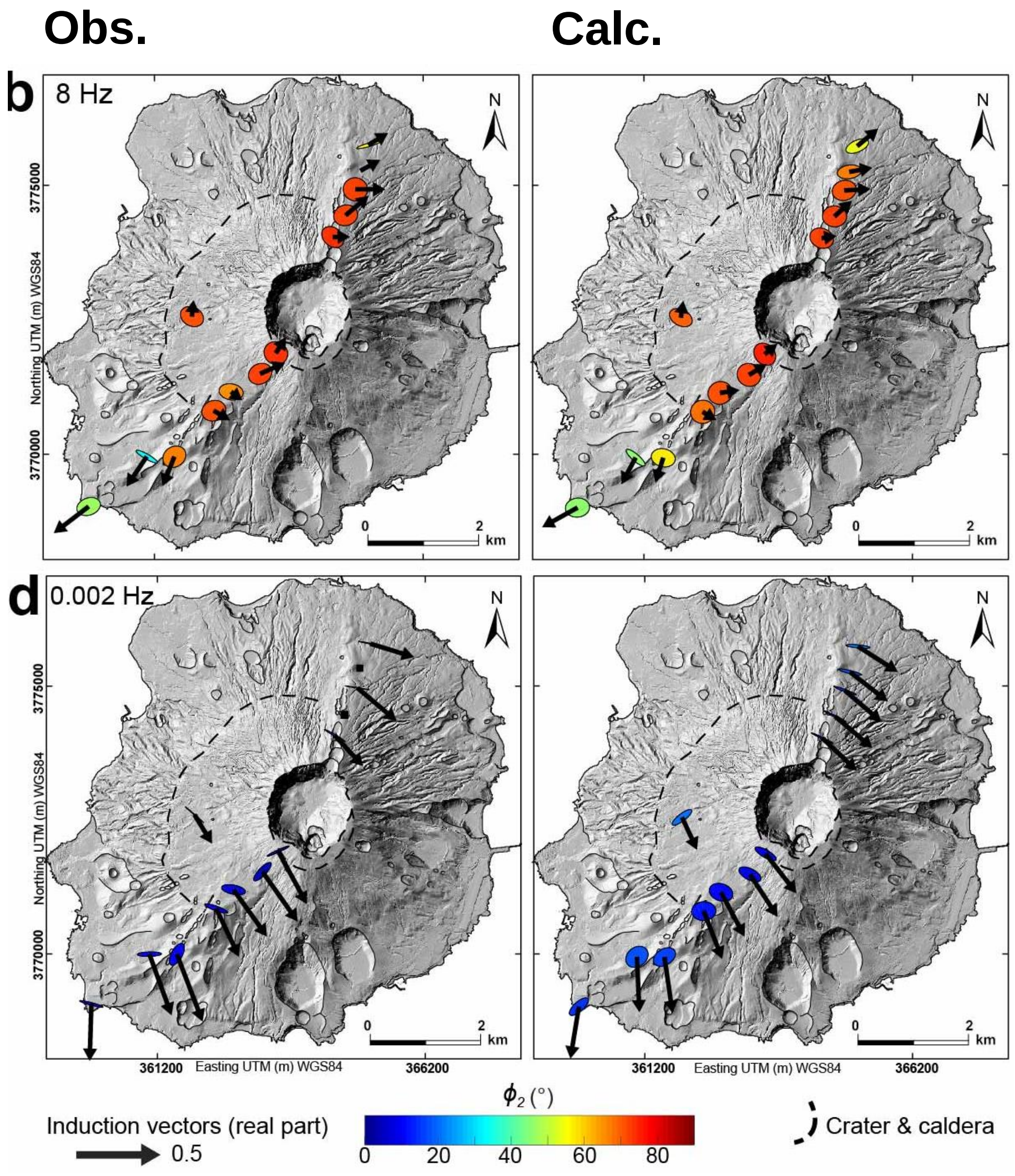

Parkinson's convention

ϕ_2= geometric mean of the phase tensor axes $= tan^{-1}(\sqrt{\phi_{max}\phi_{min}})$

$$\vec{T}real\,(f) = \left(-Real\;T_x(f), -Real\;T_y(f)\right)$$

Vectors point toward conductors

High frequencies
Conductor beneath the central part of the caldera

Low frequencies
Local bathymetry effect

Results: global overview of the resistivity model

Resistivity range: 2.5 – 2200 Ω·m

→ *consistent with 1-D model from Zlotnicki et al. 2003*

Max depth of investigation: 4.5 km below sea level (bsl)

4 units identified confirmed by 3-D forward modeling

→ detailed explanation of each unit based

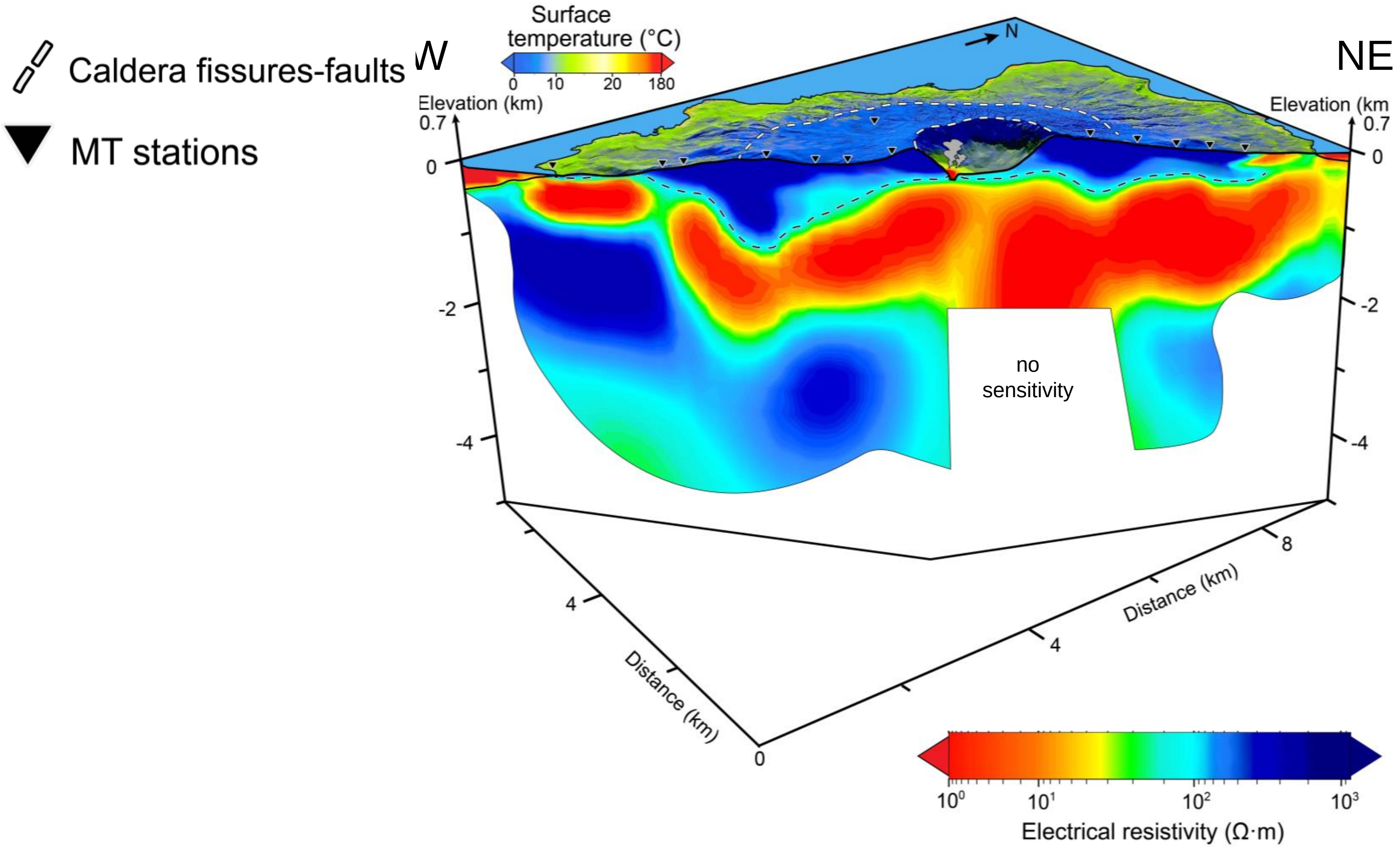

Plumbing system (1): vadose zone

1) 130 – 2200 Ω·m → unsaturated, low temperature deposits (< 15°C)

Surface – 0.7 km depth → Water table estimated with Archie's law →

Location	ϕ	S_W	T (°C)	ρ' (Ω·m)
surface	0.550	0.2	15	**2145**
~0.3 km bgs (water table)	0.444	1.0	15	**130**

$$\sigma_{rocks} = \phi^2 S_w^2 \left(\sigma_{fluids\,(T)}\right)$$

→ *Surface porosity from Nomura et al.* (2003)

→ *Surface T consistent with thermal map and meteorological temperature average*

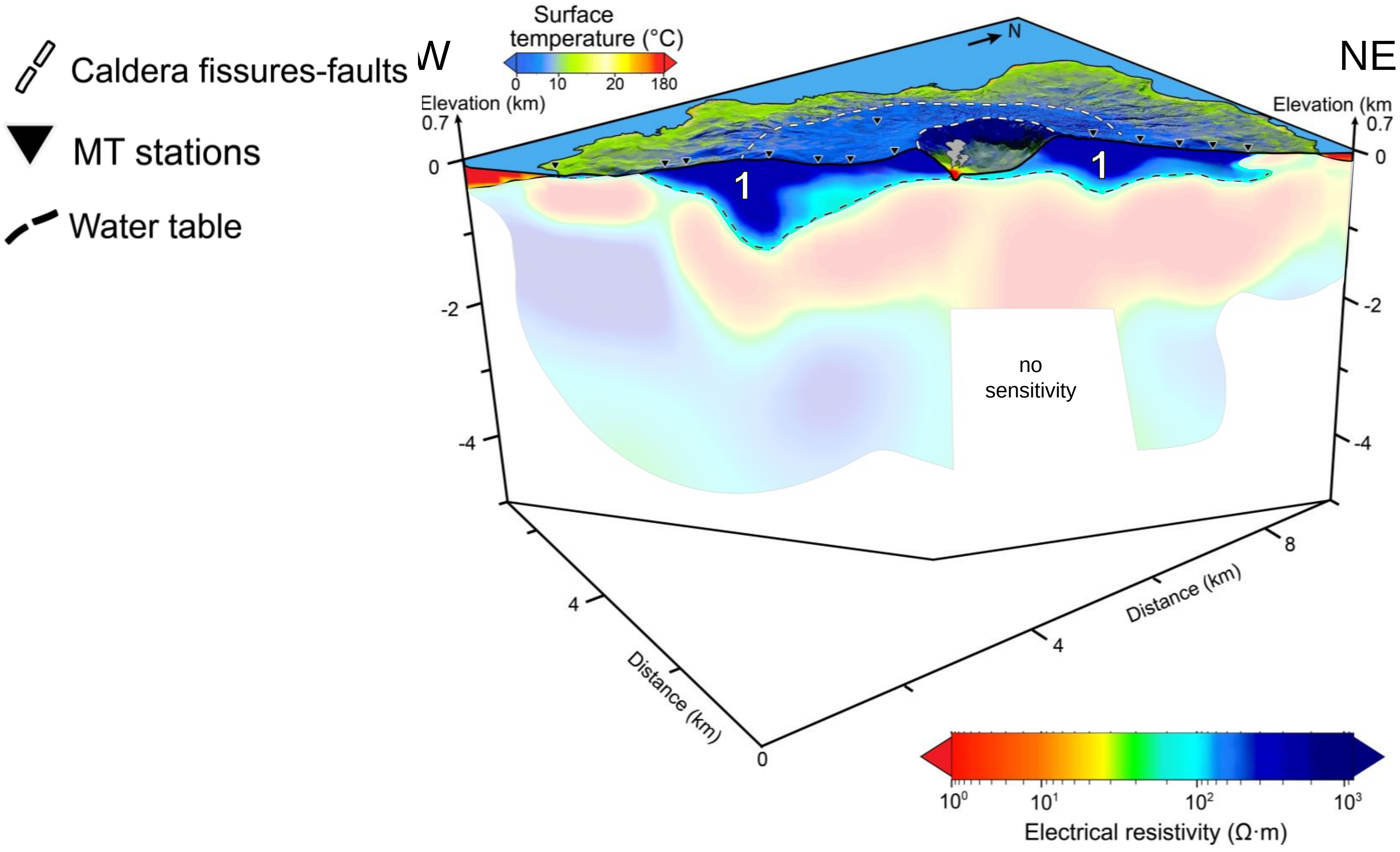

Plumbing system (2): clay cap

2) 2.5 – 30 Ω·m → water-saturated, altered rocks (up to 20 % of smectite), and high temperature (50 – 250 °C)

0 – 2 km bsl

(Yasuda et al. 2002)

Smectite < 230 °C *(Flóvenz et al. 2005)*

$$\sigma_{rocks} = \phi^2 S_w^2 \left(\sigma_{fluids\,(T)} + \sigma_{surface(T)}\right)$$

	Location	φ	Sw	T (°C)	Rock CEC (meq·100g^{-1})	ρ' (Ω·m)
a) low alteration	~1 km bsl	0.27	1.0	50	4	**26**
b) medium alteration				200	20	**2.6**
c) high alteration				250	4	**6**

Surface conductivity = 40 – 80 % of σ_{rocks}

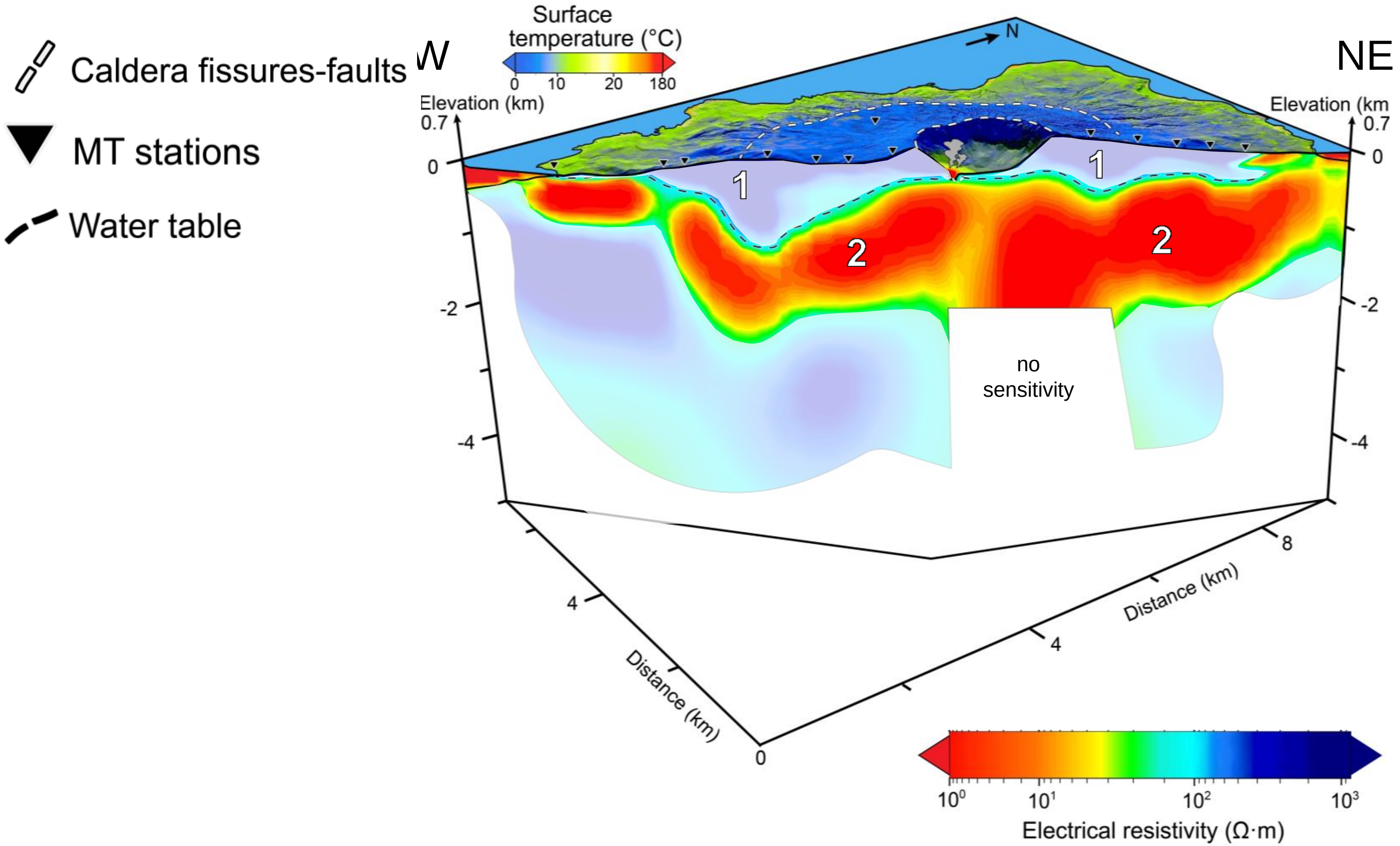

Plumbing system (2): clay cap

2) 2.5 – 30 Ω·m → water-saturated, altered rocks (up to 20 % of smectite), and high temperature (50 – 250 °C)

0 – 2 km bsl → long-period events (blue dots) around the conduit

- **Steam explosion** of liquid-dominated region *mechanism explained by Ohminato (2006) Matoza & Chouet (2010)*
  → explains the increase of water content in fumaroles

Shinohara et al., 2017
Gresse et al., 2021

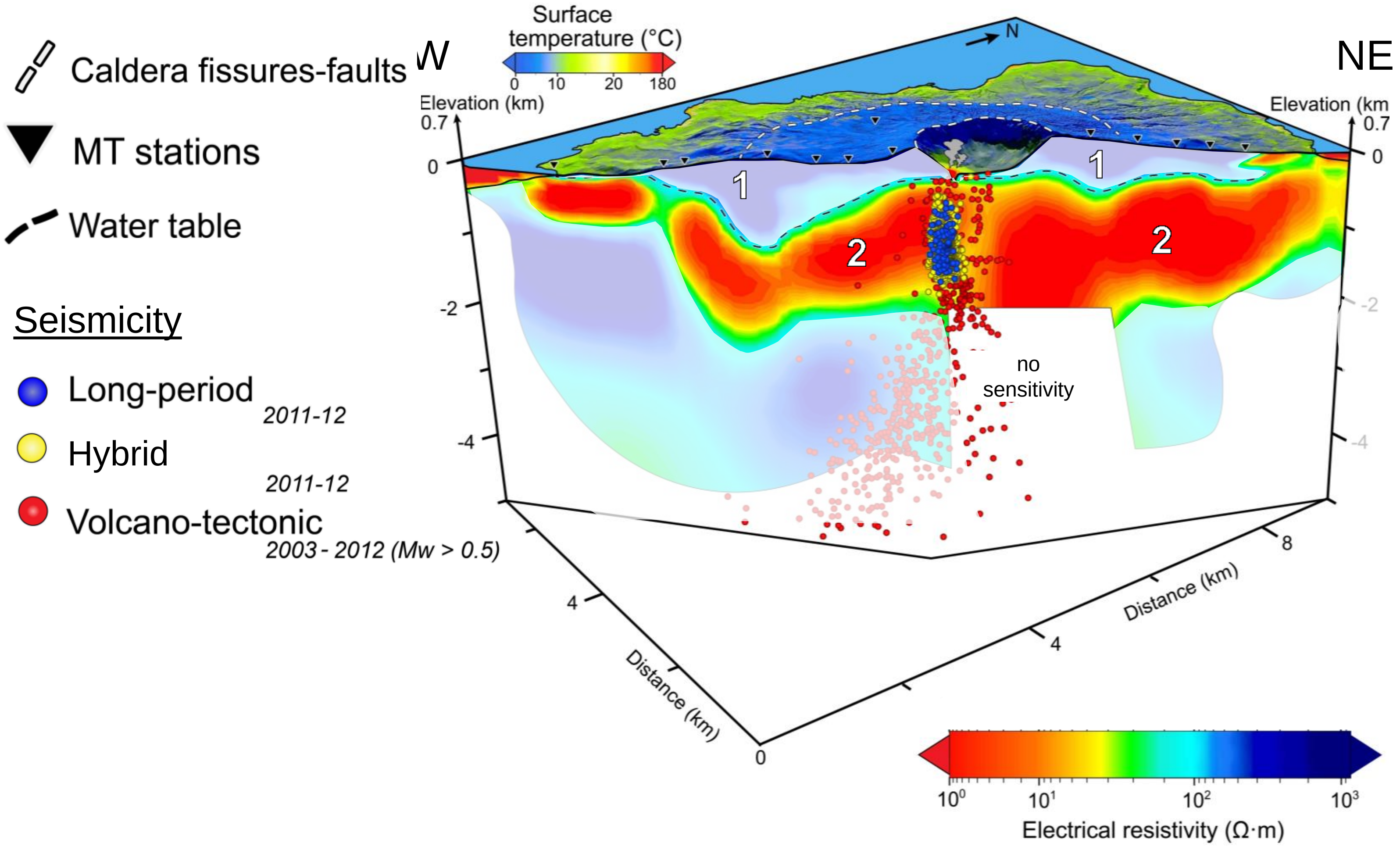

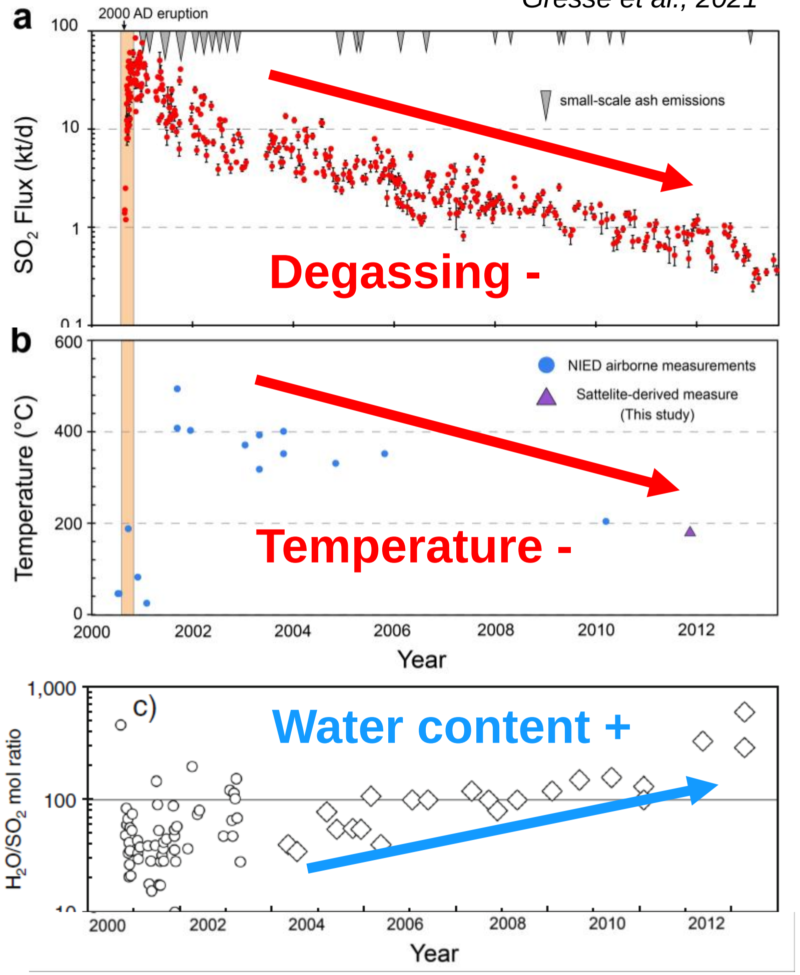

Plumbing system (3): basement rocks

3) 70–1000 Ω·m → aseismic zone, no alteration, medium temperature (<100 °C)

seabed – 2.5 km bsl

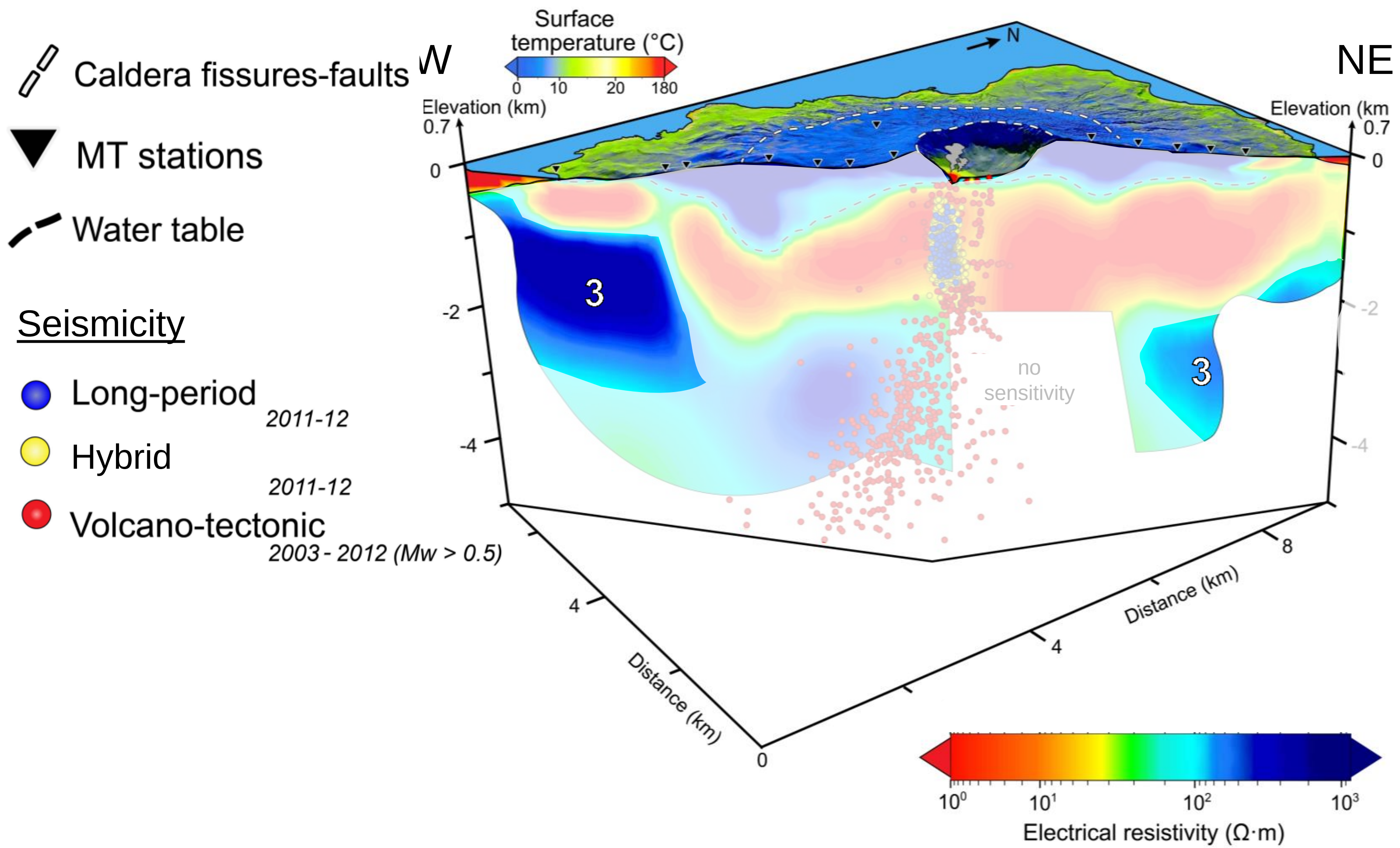

Location	φ	S_W	T (°C)	ρ' (Ω·m)
~0.3 km bsl	0.444	1.0	15	**66**
~2.5 km bsl	0.094		81	**490**

Plumbing system (4): magmatic fluids reservoir

4) 200 – 500 Ω·m: → volcano-tectonic events (red dots) → location of the ancient shallow magma chamber

2 – 4.5 km bsl → interpreted as **partially gas-saturated/supercritical fluids zone** (> 370 °C 220–300 bars)

→ could have formed after the drainage of the shallow magmatic during the 2000 eruption

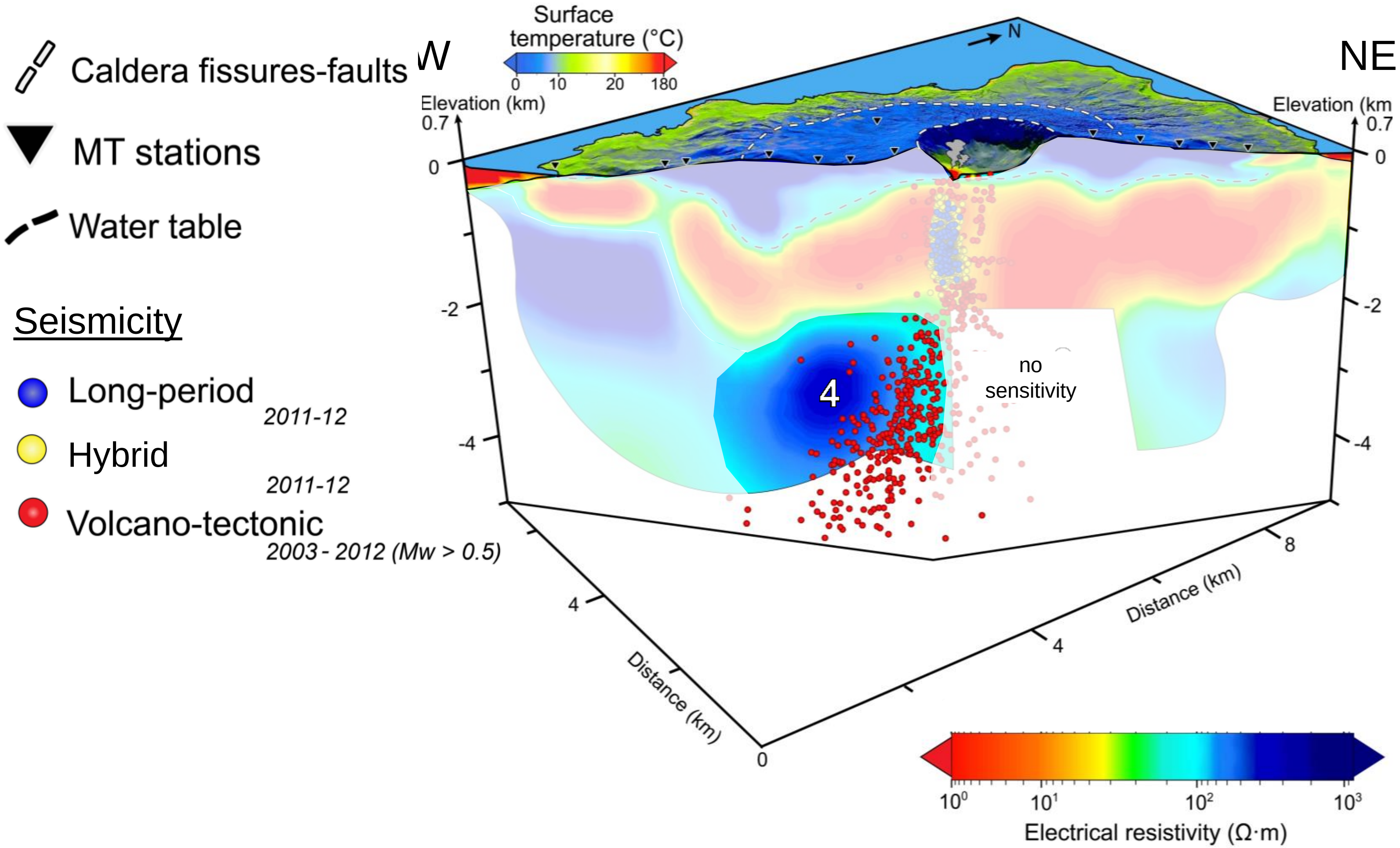

	Location	ϕ	S_W	T (°C)	ρ' (Ω·m)
a) water-saturated	~2.5 km	0.094	1.0	370	**63**
b) two-phase region			0.4	370	**395**

Plumbing system (5): fluid-flow

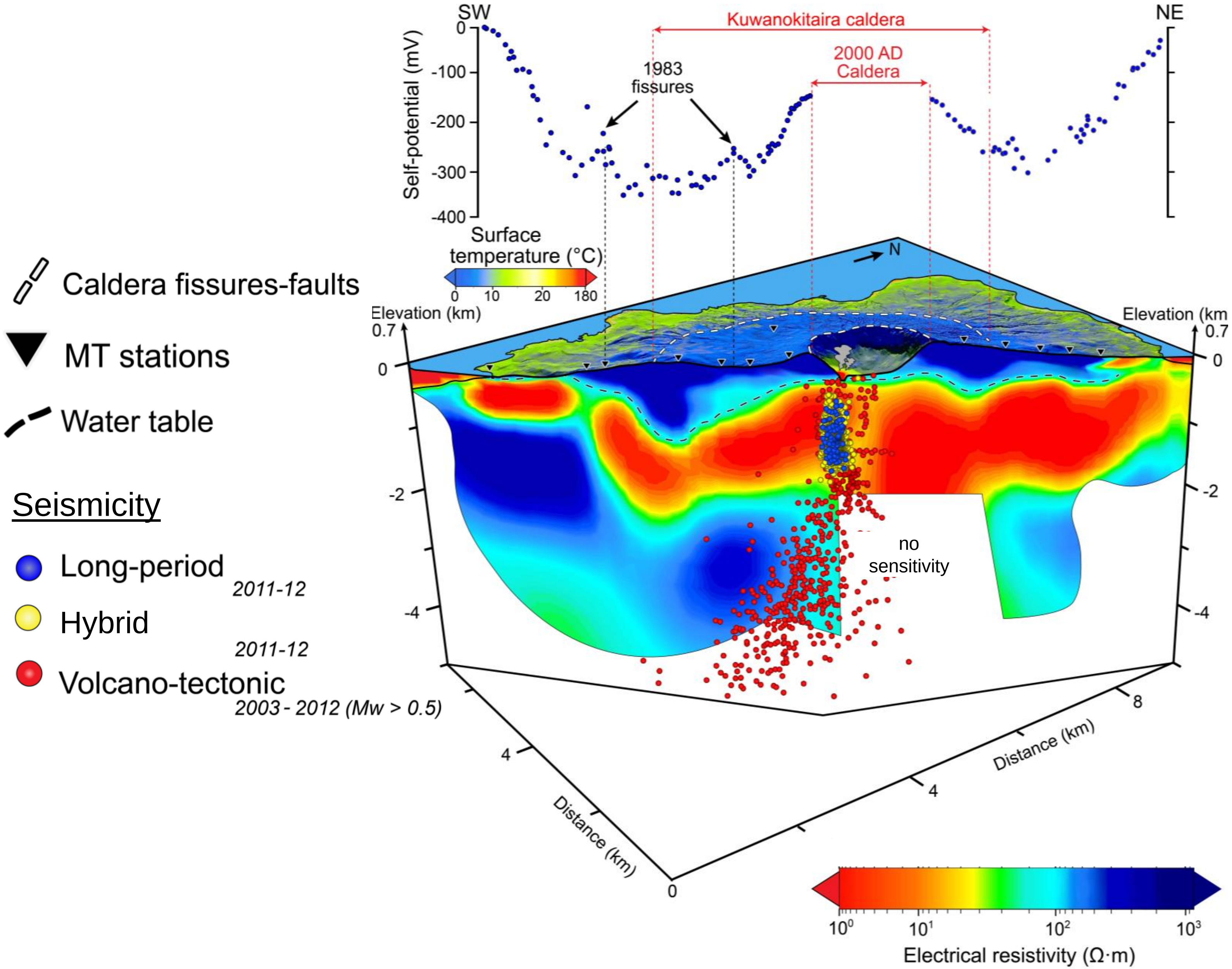

« **W-shaped** » self-potential

(Similarities with Sasai et al., 1997)

Positive anomalies

→ conductive hydrothermal plume

→ water-table upwelling near coast (hot springs)

→ 1983 fissure eruption

Negative anomalies

→ water infiltration esp. Kuwanokitaira caldera

Plumbing system (5): fluid-flow

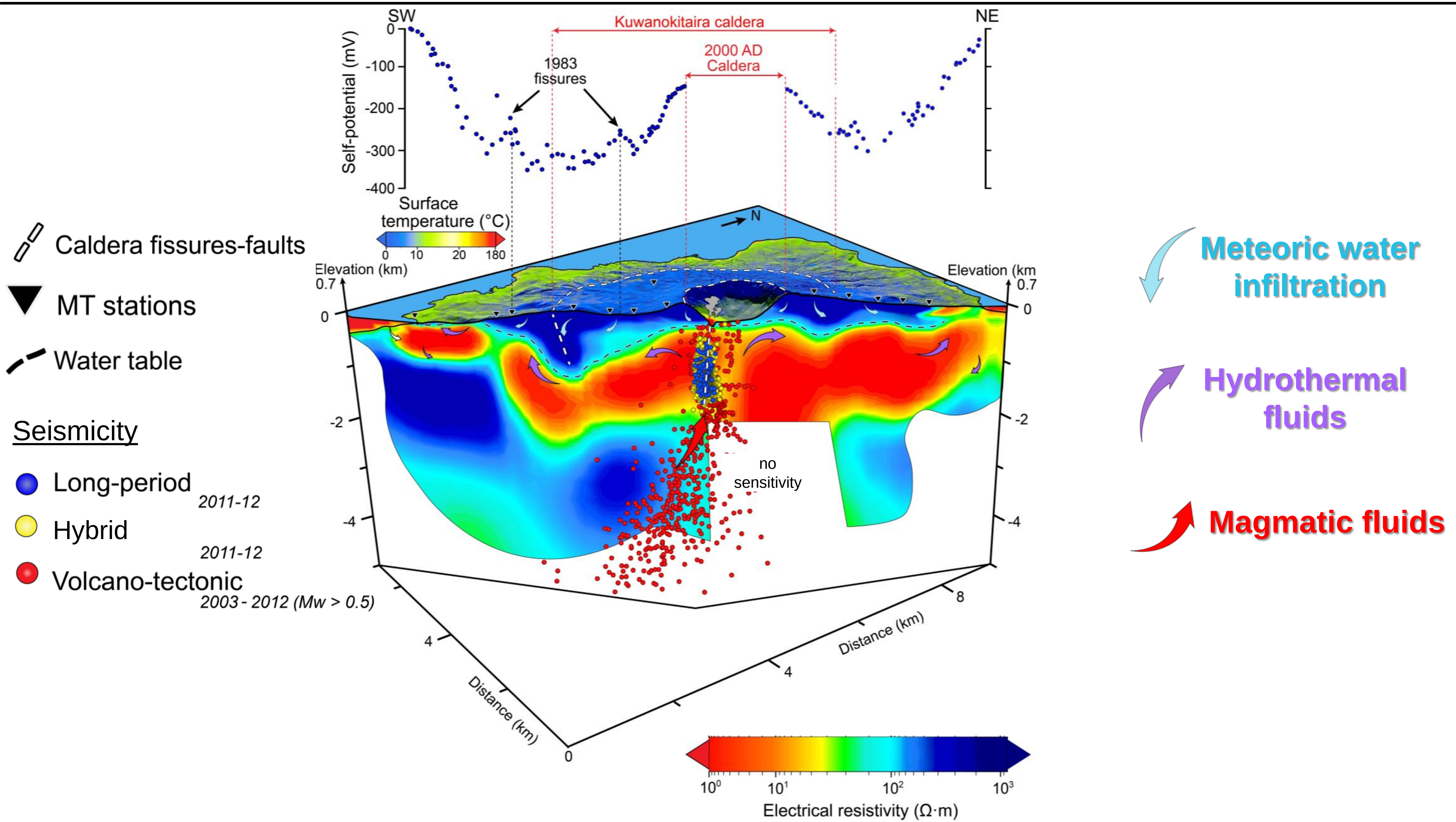

Plumbing system (6):Interpretative scheme

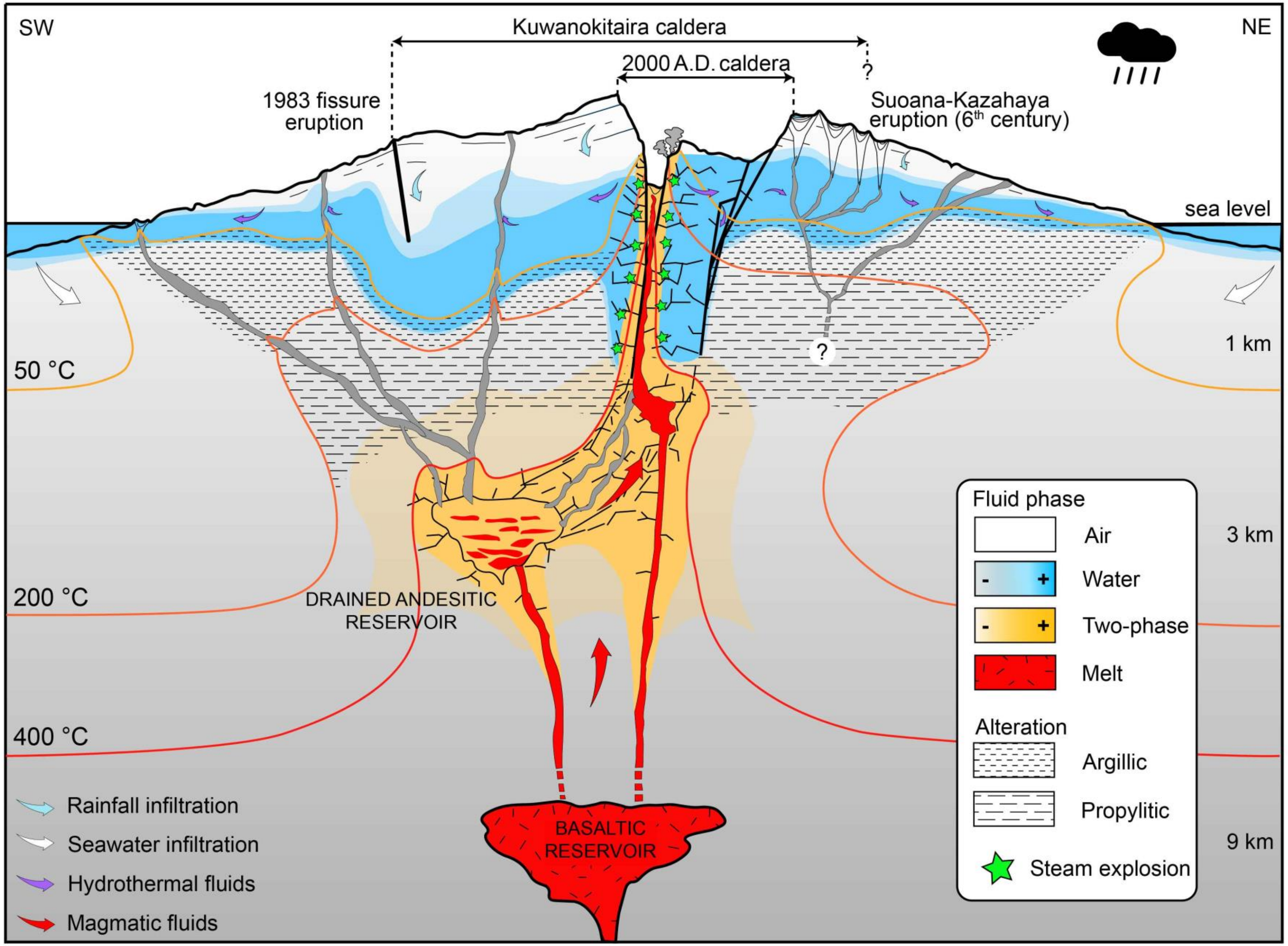

Conclusion

Plumbing system of Miyakejima volcano highlighted using a multidisciplinary approach

→ ***four geophysical methods: magnetotellurics, seismicity, self-potential, and surface thermal image***

→ **Hydrothermal-magmatic structures** characterized: rock properties, temperature, fluid content, and fluid flow

1. **Position of aquifer** defined (0–700 m depth)
   → implication for explosive/effusive eruptions

2. **Elongated clay cap**:
   → sealing the degassing activity

3. **Magmatic-hydrothermal interactions** revealed in the fractured conduit (0–2 km depth)
   → steam explosions with long period events
   → explain the water-content increase of fumaroles after 2000

Implications - Perspective

- **Investigate spatio-temporal change** until the next eruption, expected in few years
  → Resistivity, seismicity, temperature, and self-potential

- **Numerical models** to constrain these changes→ retrieve unrest mechanisms?